IEEE Access
Multidisciplinary | Rapid Review | Open Access Journal

Received July 22, 2020, accepted July 27, 2020, date of publication August 3, 2020, date of current version August 19, 2020.

Digital Object Identifier 10.1109/ACCESS.2020.3013651

Noise Suppression and Precise Phase Control of a Commercial S-Band Magnetron

SEONG-TAE HAN[1,2], (Member, IEEE), DOKYUN KIM[2], JONGSOO KIM[1], AND JONG-RYUL YANG[3], (Member, IEEE)

[1]Electrophysics Research Center, Korea Electrotechnology Research Institute, Changwon 51543, South Korea
[2]Energy and Power Conversion Engineering, University of Science and Technology, Changwon 51543, South Korea
[3]Department of Electronic Engineering, Yeungnam University, Gyeongsan 38541, South Korea

Corresponding author: Seong-Tae Han (saiph@keri.re.kr)

This research was supported by the Korea Electrotechnology Research Institute (KERI) Primary Research Program through the National Research Council of Science & Technology (NST) funded by the Ministry of Science and ICT (MSIT) (No. 20A01047).

ABSTRACT We demonstrate noise suppression and precise phase control of a commercial 2.45GHz magnetron aiming for wireless power transfer application. The impurity of the microwave spectrum was confirmed to be due to the switching frequency of 76kHz in the power supply. With the decoupling capacitor installed to the output of the high-voltage power-supply driving the magnetron, the spectral purity of the magnetron was significantly enhanced. And we achieved extreme precision in phase-control (peak-to-peak 0.3°) for the high-power (1 kW) microwave magnetron by applying the phase locking loop to the noise-suppressed magnetron system.

INDEX TERMS Wireless power transfer, magnetron, noise suppression, phase control, switching frequency.

I. INTRODUCTION

To make the space solar power system (SSPS) economically feasible that transfers electric power wirelessly via microwave to the earth after the sunlight generation on the geostationary orbit, a high-power microwave module capable of (1) few grams per unit power in the weight-power ratio and (2) 70% or higher in the DC-RF power conversion ratio, is required [1]–[13]. Magnetron is a competitive source satisfying both of the requirements, (1) to reduce launch costs and (2) to maximize energy utilization and to minimize thermal loss, among various microwave modules [2], [14].

Because of such competitiveness, magnetrons have been widely adapted in various fields such as microwave ovens of home appliances, radars, communication, medical accelerators, generation of processing plasmas, industrial heating and chemical process intensification [15]–[19]. In addition, capital cost of a magnetron is superior compared to other high-power microwave modules [20].

Magnetron devices, however, are vulnerable to harmonic and frequent spiky noise compared to other microwave modules, resulting in the instability of the phase and the frequency [21]–[23]. Consequently, such shortcomings prevent magnetrons from being employed as unit sources of a phased array system forming a spatially confined energy beam and controlling the direction of the beam precisely to realize long distance wireless power transfer systems, including the SSPS targeting from the 36,000 km above to the diameter of 100 m.

Therefore, it is necessary to study methodologies controlling and fixing the phase of magnetrons to the extent of the precision required for a phased array antenna [24]–[28].

In this article, the authors report demonstrations on extreme stabilization of the phase and the frequency of an S-band magnetron by the injection locking to prove the feasibility of magnetrons to be employed as unit sources of a phase-arrayed power-transfer system.

We report noise analysis results and methods to suppress the noise in Sec. II. In Sec. III, design and operational characteristics of the phase locking loop (PLL) to stabilize the phase of a magnetron. Conclusion follows in Section IV.

II. NOISE SUPPRESSION OF A MAGNETRON

A commercial S-band magnetron (National Electronics YJ1540) and a switching mode power supply (Alter SM445) are used for demonstrations as depicted in Fig. 1.

A. NOISE ANALYSIS

The magnetron consists of a grounded anode and the cathode emitting electrons at a negative high-voltage, where the heater power is controlled by thyristors. The low-frequency

The associate editor coordinating the review of this manuscript and approving it for publication was Shiwei Xia.

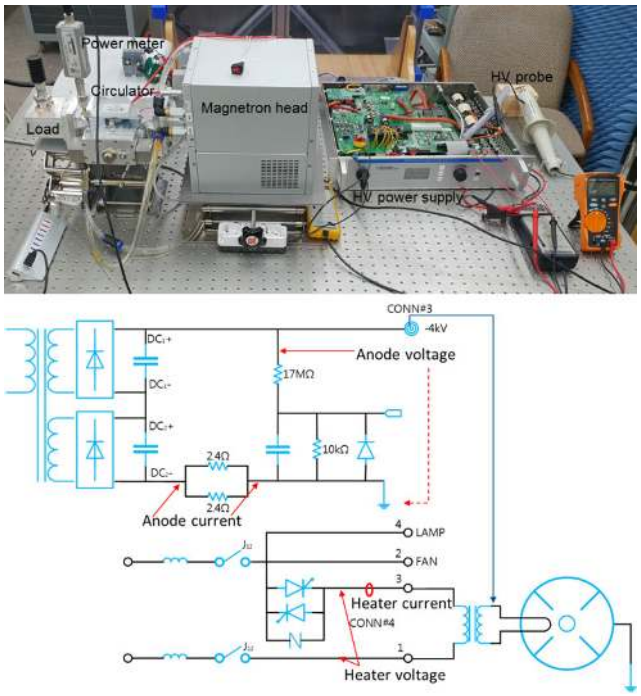

FIGURE 1. The experimental setup and the schematic diagram of the high-voltage power supply and the magnetron head.

noises from the magnetron is attributed to the modulated phase of AC heater power by the thyristors as recorded in Fig. 2 (a) and (b).

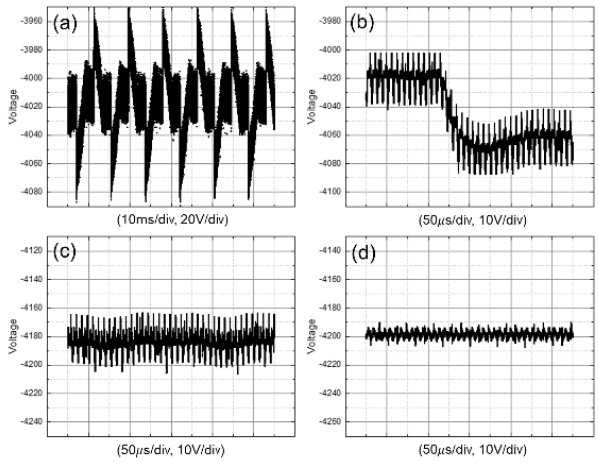

FIGURE 2. Oscilloscope trace of the anode voltages (a) for free-running with 10 ms/div, (b) for free-running with 50 μs/div, (c) for heater-off with 50 μs/div, and (d) for heater-off along with a high-voltage filter with 50 μs/div., 76-kHz noise is clearly observed in (b) and (c), and effectively removed by applying the filter.

Electrons recurring to the cathode instead of being grounded through the anode by its operation principle contributes to the temperature rise of the emitting surface of the cathode. As the result of the recurrence, the magnetron is capable of operation without an external power source to heat up the cathode. Figure 2 (c) clearly shows 76-kHz switching noise loaded in the high-voltage even when the slow noise by the heater power supply is excluded by turning off the heater power.

B. HIGH-VOLTAGE LOW-PASS FILTER

To suppress the switching noise loaded on the high voltage driving the magnetron, a high-voltage (HV) low-pass filter (LPF) with the cut-off frequency of about 300 Hz is employed. The decoupling capacitors constituting the LPF is installed to the output of the HV power supply in series as shown in Fig. 3. The overall capacitance of the decoupling capacitor is 5 μF, consisting of five capacitors with the capacitance of 25 μF, where the five resistors with the resistance of 1.22 MΩ make the voltage evenly distributed over each capacitor.

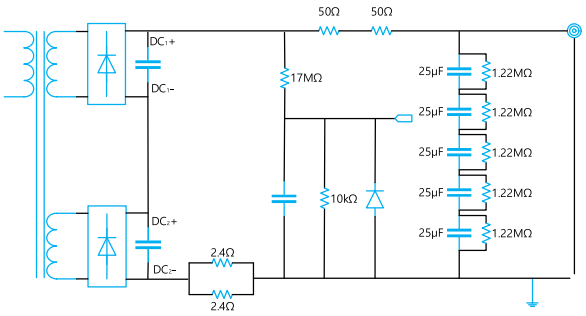

FIGURE 3. Schematic diagram of the decoupling capacitor disposed to the output of the high-voltage power supply in series.

With the help of the LPF, the 76kHz noise from the power supply was suppressed as shown in Fig. 2 (d). Also the spectral purity of the microwave was improved as presented in Fig. 4 (c) compared to the cases of free running and heater-off in Fig. 4 (a) and (b), respectively. The linewidth of

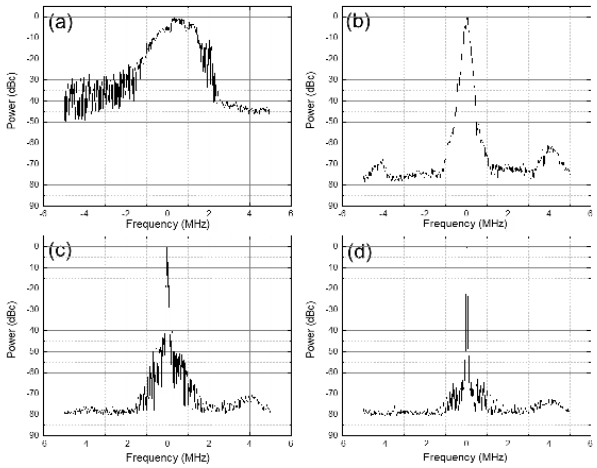

FIGURE 4. The spectral characteristics of the magnetron at the output of 1 kW in case of (a) default (free-running with heater power), (b) heater-off, (c) employment of high-voltage (HV) low pass filter (LPF) without heater, and (d) injection locking under previous conditions. (RBW: 100 kHz, VBW: 100 kHz).

the microwave spectrum was significantly enhanced though there are still minor sideband peaks below −40 dBc.

C. INJECTION LOCKING

The spectral purity in Fig. 4 (c) is still insufficient owing to the side bands attributed to the 76 kHz noise. To suppress the noise in the microwave spectrum of the magnetron further, the injection locking method was employed to the magnetron driven by the power supply equipped with the LPF when the heater power is off.

From the comparison between Fig. 4 (c) and (d), it is clear that the spectral purity is significantly enhanced, where the side bands peaks around −40 dBc in Fig. 4 (c) are suppressed down to −60 dBc as Fig. 4 (d) and the linewidth of the main signal becomes narrower by the injection of the external pure reference of 10 W.

The DC to RF conversion efficiency of the magnetron was maintained around 70% keeping the output power of 1 kW constant within the uncertainty of the power measurement. Power-added efficiency as a metric of amplifier is also similar to the conversion efficiency within 1% because the injection power was kept constant ever afterward for the injection of the PLL.

To inject the external signal generated from a signal generator (Keysight N5171B) and amplified by a power amplifier (KRF), a three-port circulator (National Electronics) terminated with a load is used. And the magnetron operates like an amplifier [24]. The power of the injection signal is maintained around 10 W so that the power gain of the amplifier is 20 dB. The injection power and the tunable bandwidth matches the estimation by Adler theory [29].

III. PHASE STABILIZATION OF A MAGNETRON

The phase of the magnetron is monitored by a phase detector (Analog Devices AD8302) with the sensitivity of 10 mV/°. The phase shifter (Analog Devices HMC 929) in front of the phase detector is inserted to keep the phase detection range of the phase detector optimum in terms of the linearity of the voltage per phase. Ten times average to minimize the effect of thermal noise, guarantees the resolution of the phase measurement down to 0.3°. The stable signal from the generator is coupled as a reference by a directional coupler, and then the phase is adjusted to the one from the magnetron by a phase shifter (Analog Devices HMC928). Figure 5 shows the schematic diagram of the experimental setup of the injection locked magnetron.

A. PHASE LOCKING LOOP (PLL) INJECTION

The phase of the magnetron corresponding to Fig. 4 (d) is presented in Fig. 6. Even only with the simple injection locking, the phase of the magnetron is stabilized within 0.5° (peak-to-peak). However, the remaining switching noise from the HV power supply is clearly observed in the phase trace of the microwave from the magnetron.

To suppress this switching noise reflected in the phase trace further, a phase locking loop (PLL) is introduced into

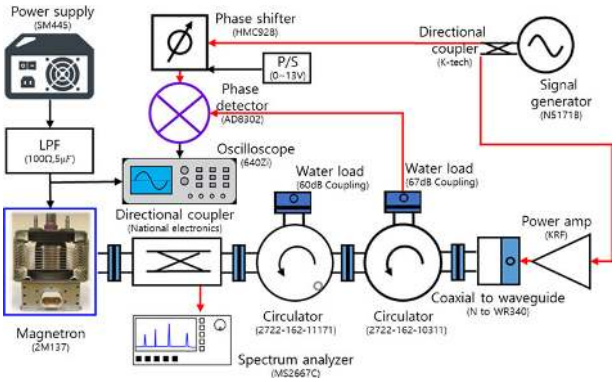

FIGURE 5. Schematic diagram of the experimental configuration for injection locked magnetron.

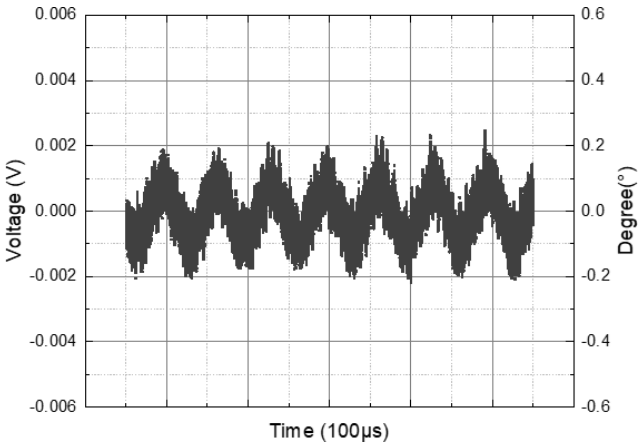

FIGURE 6. Phase stability (within 0.5° peak-to-peak) of the injection locked magnetron with PLL at the 80% of the maximum power (1 kW) after averaging out thermal noise, where the macroscopic pattern corresponds to 76 kHz as the same as the switching noise from the HV power supply.

the injection system. The basic idea of the PLL is similar to the previous studies [25]–[28]. Figure 7 shows the schematic diagram of the experimental setup of the PLL injection stabilizing the phase of the magnetron to the extreme.

The Wilkins power divider is integrated in the PLL circuit board to divide the power of the reference into the phase shifters for both of the phase detection and the phase adjustment. The other phase shifter in front of the double balanced mixer (Mini-Circuits SYM-25DLHW) controls the phase of the injection locking signal. The double balanced mixer is a phase comparator of microwaves from the magnetron and the reference, and produces a voltage proportional to the difference.

The overall response time of the PLL was assumed to be about 200 ns considering the filling time of electrons in the magnetron resonator.

B. PLL CIRCUIT

The PLL circuit (enclosed with a box in Fig. 7) consists of the Wilkins power divider distributing the microwave reference both to a phase shifter locking the phase of the magnetron

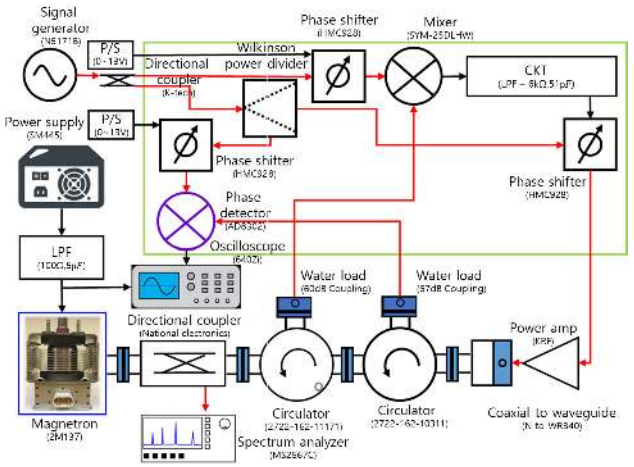

FIGURE 7. Experimental configuration of injection locking with the phase locking loop (PLL). PLL mainly consists of a double balanced mixer detecting the phase difference between the reference and the magnetron and a control circuit (CKT) producing the voltage to adjust the phase of the phase shifter.

in the desired one and to a double balanced mixer detecting the phase difference between the reference signal and the microwave from the magnetron, and a control circuit (CKT) producing the voltage to adjust the phase of the phase shifter accordingly.

Figure 8 shows the schematic diagram of the circuit (CKT). The voltage from the double balanced mixer is added to the offset voltage to operate the phase shifter in the optimum. The overall voltage is amplified with the inverted polarity and a designed gain, and fed to the phase shifter (Analog Devices HMC928) by the operational amplifier (Texas Instrument OPA828). A buffer (voltage follower) is placed between the phase shifter and the integrator to maintain the voltage regardless of the load.

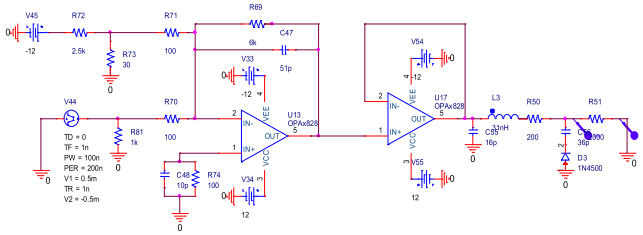

FIGURE 8. The schematic diagram of the CKT. The voltage to adjust the phase is produced by the inverting amplifier and offset bias, then applied to the phase shifter through the buffer. The operational amplifiers employed in the PLL has 150V/μs of slew rate and 45 MHz of open gain bandwidth. Resistances and capacitances were determined considering the time constant of the circuit and optimized by PSpice simulation.

Figure 9 and 10 show the OrCAD drawing and a fabricated PCB of the PLL circuit, respectively. To shield the effect of any external noise, the circuit is placed in the aluminum housing.

C. PRECISE CONTROL OF THE PHASE

A down-conversion setup mixing the magnetron signal with a well-defined reference is employed to monitor the jittering

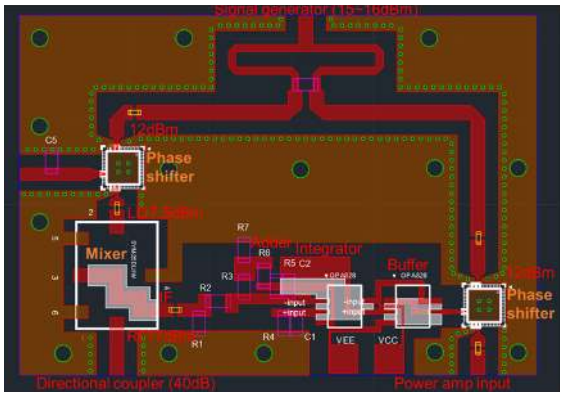

FIGURE 9. OrCAD drawing of the PLL circuit, corresponding to the enclosed box in Fig.7.

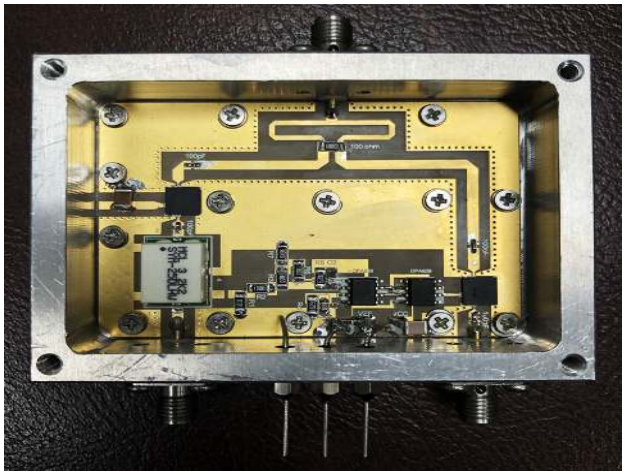

FIGURE 10. Fabricated PCB of the PLL, corresponding to the enclosed box in Fig.7.

of the microwave from the magnetron in time-domain at an intermediate frequency (IF) below 50-MHz. A wideband synthesizer (Analog Devices ADF4351) and a low noise amplifier (Kbell AMP-W) is used as the reference, where the phase noise of the reference is stabilized to −100 dBc at 1 kHz.

Figure 11 shows the IF traces with an oscilloscope over time span of 50 ns, where the HV LPF is applied to all cases. When the magnetron runs without any measure, the phase noise is reflected as the serious jittering noise as shown in Fig. 11 (a). When the heater power is off, the jittering noise is reduced much as shown in Fig. 11 (b). Additionally, when the injection locking is employed, the jittering noise is reduced significantly as shown in Fig. 11 (c) and (d).

Figure 11. (d) is the phase trace when the PLL is added to the injection locking though the result looks similar to Fig. 11 (c). To make the difference clear, the IF traces are monitored over the time span of 1 ns, corresponding to about 15° in the phase of the microwave. As Fig. 12 (a) and (b) show, the reduction of the jittering noise is qualitatively reduced.

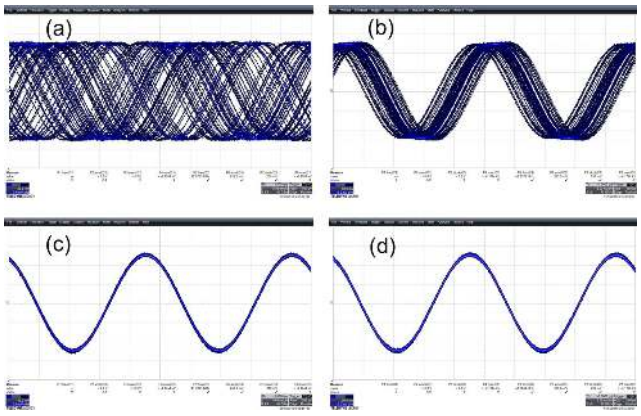

FIGURE 11. Jittering of magnetron oscillation over the time span of 50 ns in case of (a) free-running with heater on, (b) heater-off, (c) injection only and (d) PLL, where the microwaves from the magnetron oscillation were down-converted to 41 MHz by a mixer and a precise reference.

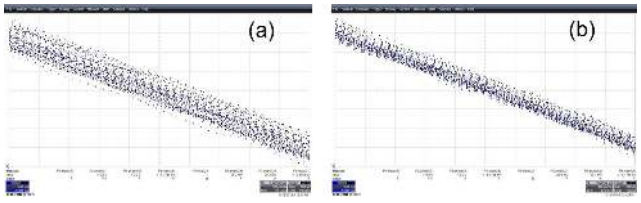

FIGURE 12. Jittering of magnetron oscillation in case of (a) injection only and (b) PLL over the time span of 1 ns corresponding to about 15° in phase.

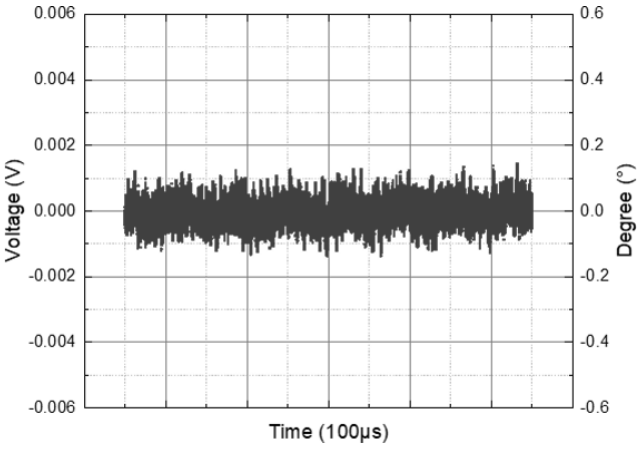

FIGURE 13. Phase stability (about 0.3° peak-to-peak) of the injection locked magnetron with PLL at the 80% of the maximum power (1 kW) after averaging out thermal noise.

Figure 13 shows the effect of the PLL quantitatively. From the comparison with Fig. 6, it should be clearly noticed that the macroscopic pattern corresponding to the 76 kHz switching noise in Fig. 6, disappears in Fig. 13. And the phase stability of around 0.3° peak-to-peak within the resolution of the phase detector is achieved. The phase stability in root-mean-square (rms) is 0.035°, which is the best value in the short period of time (100 μs), to the authors' knowledge, enough to be applied instead of a klystron to a linear accelerator for X-ray free electron lasers [30].

The phase of the magnetron was stabilized to the extreme as shown in Fig. 13, and the phase of the injection locked magnetron was adjusted from −180° to 180° by the phase shifter inserted in front of the double balanced mixer.

Long-term drift of the phase was monitored as presented in Fig. 14, where the peak-to-peak stability of the phase around ±1°. In this case, the number of data points prevent the authors from applying the average to minimize the thermal noise effect. By assuming the reduction factor of 5 convinced from the previous case, the phase stability over the long-term may be within around 0.4° (±0.2°). If we analyze the dada points over the long time period statistically as other groups [25]–[28], similar level of the stability is obtained.

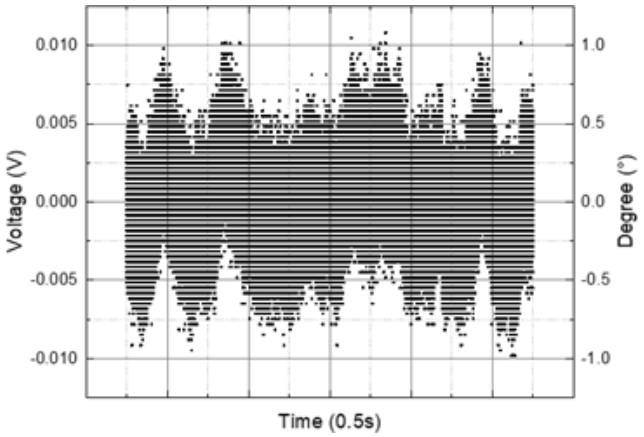

FIGURE 14. Drift of the phase for the long time of 500 ms.

Figure 15 shows the long-term drift of the voltage from the phase detector and the anode voltage, where the voltage from the phase detector is the exact replication of the anode-voltage. The variation of the anode voltage is to maintain the power from the HV power supply at a constant value due to the internal feedback algorithm. The authors are pretty sure such a long-term drift could be further suppressed by employing or developing a HV power supply regulated more stably.

FIGURE 15. Long-term drift of the phase (green) and the anode voltage (yellow), which is exact replication of the anode-voltage variation to maintain the anode-current at a constant value.

IV. CONCLUSION

In summary, extreme stabilization of the phase (0.3° peak-to-peak and 0.035° in rms) and the frequency (below −60 dBc of noise floor) of a commercial S-band magnetron driven by the power supply with the switching frequency of 76kH suppressed further and the heater power off, was realized by locking with external signal along with the PLL. This demonstration on improving the spectral purity of an S-band magnetron to the satisfaction of the tight requirements of the phased array system, proves the feasibility of a magnetron as a promising candidate for the microwave power units for a long-distance wireless power transfer system.

ACKNOWLEDGMENT

The authors would like to thank Ms. Y. Heo and Prof. J. Choi with Kwangwoon University for managing the PCB fabrication in the part of the PLL.

REFERENCES

[1] W. C. Brown, "Satellite power system (SPS) magnetron tube assessment study," Nat. Aeronaut. Space Admin., Washington, DC, USA, Tech. Rep. 3383, 1981.
[2] P. E. Glaser, "Feasibility study of a satellite solar power station," NASA, Washington, DC, USA, Tech. Rep. CR-2357, 2000.
[3] P. E. Glaser, "Power from the sun: Its future," *Science*, vol. 162, no. 3856, pp. 857–861, Nov. 1968.
[4] W. C. Brown and E. E. Eves, "Beamed microwave power transmission and its application to space," *IEEE Trans. Microw. Theory Techn.*, vol. 40, no. 6, pp. 1239–1250, Jun. 1992.
[5] E. Ackerman, "Japan demoes wireless power transmission for space-based solar farms," in *Proc. IEEE Spectrum*, Mar. 2015, pp. 1–7.
[6] S. Sasaki, K. Tanaka, and K.-I. Maki, "Microwave power transmission technologies for solar power satellites," *Proc. IEEE*, vol. 101, no. 6, pp. 1438–1447, Jun. 2013.
[7] N. Shinohara, "Beam control technologies with a high-efficiency phased array for microwave power transmission in japan," *Proc. IEEE*, vol. 101, no. 6, pp. 1448–1463, Jun. 2013.
[8] P. Jaffe and J. McSpadden, "Energy conversion and transmission modules for space solar power," *Proc. IEEE*, vol. 101, no. 6, pp. 1424–1437, Jun. 2013.
[9] B. Strassner and K. Chang, "Microwave power transmission: Historical milestones and system components," *Proc. IEEE*, vol. 101, no. 6, pp. 1379–1396, Jun. 2013.
[10] A. Nagahama, T. Mitam, N. Shinohara, N. Tsuji, K. Fukuda, Y. Kanan, and K. Yonemoto, "Study on a microwave power transmitting system for mars observation airplane," in *Proc. IEEE MTT-S Int. Microw. Workshop Ser. Innov. Wireless Power Transmiss., Technol., Syst., Appl.*, May 2011, pp. 63–66.
[11] W. Johnson, K. Dahlburg, B. Bartolo, W. Dorsey, D. Gubser, P. Jenkins, N. Smith, W. Boncyk, M. Brown, D. Huber, and P. Jaffe, "Space-based solar power: Possible defense applications and opportunities for NRL contributions," Nav. Res. Lab., Washington, DC, USA, Tech. Rep. NRL/FR/7650–09-10,179, 2009.
[12] N. Shinohara and H. Matsumoto, "Research on magnetron phased array with mutual injection locking for space solar power satellite/station," *Electr. Eng. Jpn.*, vol. 173, no. 2, p. 21 2010.
[13] N. Shinohara, "Applications of WPT," in *Wireless Power Transfer via Radiowaves*. Hoboken, NJ, USA: Wiley, 2014.
[14] R. J. Trew, "SiC and GaN transistors–is there one winner for microwave power applications?" *Proc. IEEE*, vol. 90, no. 6, pp. 1032–1047, Jun. 2002.
[15] J. M. Osepchuk, "The magnetron and the microwave oven: A unique and lasting relationship," in *Proc. Int. Conf. Origins Evol. Cavity Magnetron*, Apr. 2010, pp. 19–20.
[16] J. Li, Z. Yao, L. Ye, and P. Guan, "Design of magnetron transmitter for Doppler weather radar," *Proc. Int. Conf. Meteorol. Observat. (ICMO)*, 2019, pp. 28–31.
[17] J. N. Burghartz, "Vacuum device applications," in *Guide to State-of-the-Art Electron Devices*. Hoboken, NJ, USA: Wiley, 2013.
[18] H. Zhang, R. Yang, Y. He, A. Foudazi, L. Cheng, and G. Tian, "A review of microwave thermography nondestructive testing and evaluation," *Sensors*, vol. 17, no. 5, p. 1123, May 2017.
[19] S. Dábrowska, T. Chudoba, J. Wojnarowicz, and W. Åojkowski, "Current trends in the development of microwave reactors for the synthesis of nanomaterials in laboratories and industries: A review," *Crystals*, vol. 8, no. 10, p. 379, Sep. 2018.
[20] H. Wang, T. Plawski, and R. A. Rimmer, "Simulation study using an injection phase-locked magnetron as an alternative source for SRF accelerators," in *Proc. 6th Int. Particle Accel. Conf.*, Oct. 2015, pp. 1–7.
[21] W. C. Brown, "The high signal to noise ratio of magnetrons and evidence of negative feedback to control it," *Proc. 1st Int. Workshop Cross-Field Devices*, 1995, pp. 1–4.
[22] T. Mitani, N. Shinohara, H. Matsumoto, and K. Hashimoto, "Experimental study on oscillation characteristics of magnetron after turning off filament current," *Electron. Commun. Jpn.*, vol. 86, no. 5, pp. 1–9, May 2003.
[23] I. K. Baek, M. Sattorov, R. Bhattacharya, S. Kim, D. Hong, S. H. Min, and G. S. Park, "Origin of sideband and spurious noises in microwave oven magnetron," *IEEE Trans. Electron Devices*, vol. 64, no. 8, pp. 3413–3420, Aug. 2017.
[24] W. C. Brown, "The magnetron—A low noise, long Life amplifier," *Appl. Microw.*, vol. 117, p. 5, Jan. 1990.
[25] B. Yang, T. Mitani, and N. Shinohara, "Experimental study on a 5.8 GHz power-variable phase-controlled magnetron," *IEICE Trans. Electron.*, vol. E100.C, no. 10, pp. 901–907, 2017.
[26] I. Tahir, A. Dexter, and R. Carter, "Frequency and phase modulation performance of an injection-locked CW magnetron," *IEEE Trans. Electron Devices*, vol. 53, no. 7, pp. 1721–1729, Jul. 2006.
[27] I. Tahir, "Frequency and phase locking of a CW magnetron: With a digital phase locked loop using pushing characteristics," Doctoral dissertation, Eng. Dept., Lancaster Univ., Lancaster. U.K., 2008.
[28] Z. Liu, X. Chen, M. Yang, K. Huang, and C. Liu, "Experimental studies on a 1-kW high-gain *S* -Band magnetron amplifier with output phase control based on Load–Pull characterization," *IEEE Trans. Plasma Sci.*, vol. 46, no. 4, pp. 909–916, Apr. 2018.
[29] R. Adler, "A study of locking phenomena in oscillators," *Proc. IRE*, vol. 34, no. 6, pp. 351–357, Jun. 1946.
[30] M. H. Yoon, S. J. Park, E. S. Kim, W. H. Hwang, and D. E. Kim, "Accelerating device for next generation radiation (in Korean)," *Phys. High Technol.*, vol. 18, pp. 6–19, Oct. 2009.